Colloquia: IFA 2010

Three-dimensional compositional mapping using multiple energy X-ray computed tomography

M. Endrizzi

Dipartimento di Fisica, Università di Siena - Via Roma 56, 53100 Siena, Italy
INFN, Sezione di Pisa - 56127 Pisa, Italy

Summary. — When a microstructure contains finer details than the X-ray computed tomography (CT) spatial resolution, the conventional techniques based on segmentation become inadequate for separating the materials composing the sample. Data-constrained modeling overcomes this problem using multiple CT data sets acquired with different X-ray beam energies. The volume fractions of the materials contained into a single voxel are then determined by solving a linear system. The ill-conditioned nature of the linear system reflects into a high sensitivity to the noise. An alternative approach to the direct solution of the linear system, based on the iterative application of the Expectation-Maximization algorithm, is here presented. Different noise conditions are investigated for a random-generated single-voxel problem and for a more complex numerical phantom.

PACS 87.59.-e – X-ray imaging.
PACS 81.70.Tx – Computed tomography.

1. – Introduction

X-ray CT has been widely used for determining microstructures [1]. The application of segmentation techniques to the CT data set, for extracting the three-dimensional distribution of different materials, requires the assumption that a unique material is contained into each voxel. This may not be valid for rock samples: they can contain porosity on the sub-micron scale which is beyond the resolution of common commercial CT scanners [2, 3].

A data-constrained modeling (DCM) approach allows to relax the requirement that each voxel contains only one material and enables the recovery of the volume fraction information from multiple CT data sets [4, 5]. Following a case study of interest already presented [6], the attention is focused on the specific problem of determining the volume fractions for a sample composed by three materials, namely void, quartz and kaolinite. Those components of sandstone have similar X-ray absorption properties and the mapping of the materials by threshold segmentation of the CT images would be difficult [6].

Instead of directly solve the linear system obtained using DCM, the solution is computed by means of the iterative application of the Expectation-Maximization (EM) algorithm. The method is studied on a single-voxel randomly generated problem and it is subsequently applied to a numerical phantom.

2. – Method

DCM approaches the problem of determining the volume fractions of multiple known materials in the following way. A number of CT scans, acquired at different X-ray beam energies, represent the input of the method. The knowledge of the materials that compose the sample allows to write, for each voxel, the linear system

$$(1) \qquad\qquad\qquad U = AW$$

that relates the volume fractions W to the measured attenuation coefficients U [6]. U_m are the absorption coefficients measured with the CT scan for $m = 2 \ldots M$ different energies, $U_1 = 1$ by definition imposes that the sum of the various fraction is normalized to 1. W_n are the volume fractions of $n = 1 \ldots N$ different known materials. The matrix A_{mn} contains the absorption coefficient of the n-th material at the m-th energy ($A_{1n} = 1$, $\forall\, n$). Two basic assumptions are required:

– the total volume of the voxel is equal to the sum of the materials volume fractions,

– the total attenuation of the X-rays in one voxel is the sum of the attenuation of each material, weighted with its fraction.

A solution of the linear system (1) can be obtained by the iterative application of the set of equations (EM algorithm [7,8, p. 184]):

$$(2) \qquad\qquad \begin{cases} W_n^{k+1} = W_n^k f_n, \\[2mm] f_n = \dfrac{\sum_m A^t{}_{nm} \dfrac{U_m}{\sum_{n'} A_{mn'} W_{n'}^k}}{\sum_m A^t{}_{nm}}, \end{cases}$$

k is the number of iterations and A^t is the transpose of A. The initial guess is to assign equal volume fractions for each material ($W_n^0 = 1/N$). The explicit form of the matrix A of our problem is

$$(3) \qquad\qquad A = \begin{bmatrix} 1 & 1 & 1 \\ 0 & 2.2499 & 1.9562 \\ 0 & 0.8394 & 0.7703 \end{bmatrix},$$

it contains the attenuation coefficient of void, quartz (SiO_2, density 2.65 ($g\,cm^{-3}$)) and kaolinite ($Al_2Si_2O_5(OH)_4$, density 2.6 ($g\,cm^{-3}$)) at the energies of 30 and 50 keV [6].

3. – Single-voxel problem

The first step is to consider only a single voxel. The volume fractions are randomly generated and this vector is our exact solution W^{exact}. The exact measurements vector U^{exact} is computed and different amounts of noise are added. The

TABLE I. – *Comparison between the exact and the optimum solutions, the relative error (percent) with respect to the exact solution is reported in brackets.*

	Exact	Noiseless	$\sigma = 0.1\%$	$\sigma = 0.5\%$	$\sigma = 1\%$	$\sigma = 5\%$	$\sigma = 10\%$
void	0.1562	0.1562(0.0003)	0.157(0.20)	0.156(0.17)	0.15(5.1)	0.19(21)	0.24(57)
quartz	0.3067	0.3067(0.0011)	0.306(0.07)	0.307(0.05)	0.31(1.5)	0.41(34)	0.25(17)
kaolinite	0.5371	0.5371(0.0007)	0.537(0.03)	0.540(0.02)	0.54(0.6)	0.40(25)	0.50(6.7)

perturbations are randomly extracted from a normal distribution with 0 mean and $\sigma = \{0.1\%, 0.5\%, 1\%, 5\%, 10\%\}$ times the value of the measurement.

In this simulation study the exact solution is known, this allows to evaluate the convergence properties of the method. Without any noise contribution to the data the algorithm is expected to converge to the exact solution. In the presence of noise the iteration typically converges for a certain number of iterations and after this point the approximation starts to diverge from the exact solution. This behavior is called semi-convergence [8, p. 110]. These semi-convergence properties are evaluated using the root square error as a figure of merit:

$$(4) \qquad L(k) = \sqrt{\sum_{n=1}^{N} \left(W_n^{\mathrm{exact}} - W_n^k \right)^2}.$$

Starting from a convergence situation in the noiseless case, less and less accurate optimum ($L(k)$ is minimum) approximation are obtained. These optimum solutions $W^{\bar{k}}$ are reported in table I.

4. – Numerical phantom and CT data simulation

To explore the performances of the algorithm when a large number of voxels has to be analyzed, a numerical phantom has been used. It is composed by a matrix of quartz with void and kaolinite inclusions allowing mixing of the materials at the interfaces (two materials at a time). The sample is cylindrical, with diameter 4 mm and the image has 200×200 pixels. The CT data acquisition is then simulated for the two monochromatic energies of 30 and 50 keV using 720 parallel-beam projections over 180 degrees (0.25 degree steps). A simulated photon counting statistical noise of various intensities $\{0.1\%, 0.4\%, 0.8\%, 1\%\}$ is added to the projected intensity distributions. The noisy projections are reconstructed with the conventional Filtered Back Projection CT reconstruction algorithm using a dedicated software [9] (fig. 1).

The CT scans are then analyzed slice by slice. Equations (2) are then iterated simultaneously for each voxel contained into a slice. In this way we obtain the three-dimensional distribution of the volume fractions of material that compose the phantom. The quality of the computed distribution of volume fractions is quantified by means of a cross-correlation value. The cross-correlation is defined as

$$(5) \qquad Cc^m = \frac{1}{V-1} \sum_{ij} \frac{(W_m^{ij} - \bar{W}_m^{ij})(E_m^{ij} - \bar{E}_m^{ij})}{\sigma_W \sigma_E},$$
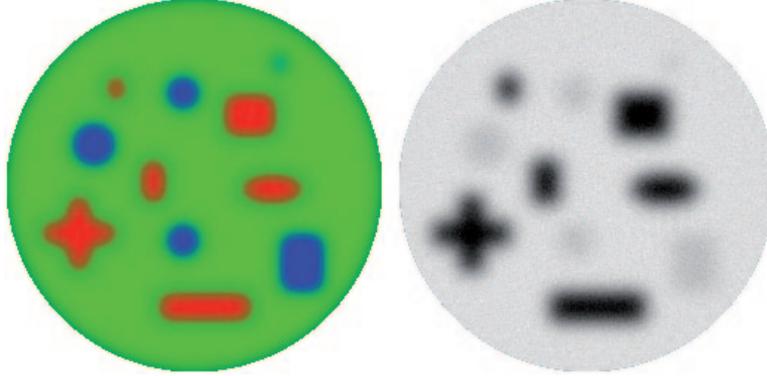
Fig. 1. – (Colour on-line) RGB representation of the exact fractions (R = void, G = quartz, B = kaolinite) and simulated CT scan at 30 keV with 0.4% photon counting statistical noise.

where the index m covers the different materials, W_m^{ij} represent the volume fraction of the material m computed at the position (i, j) into the slice and E_m^{ij} is the exact volume fraction, for the same material at the same position. $\bar{E}_m^{ij}$ is the average value of E and σ_E its standard deviation. This cross-correlation is computed after each iteration. The results, in the 0.1% and 1% noise cases, are plotted in fig. 2.

In order to evaluate the possibility to apply the method in a hypothetical real experiment a stopping rule based on the discrepancy principle [10] has been used. After each iteration k, the normalized L_2 distance between the slice that can be computed using the volume fractions and the measured distribution of attenuation coefficients obtained through CT reconstruction is computed. This quantity (residual) is expected to be a decreasing function of the number of iterations. When the residual becomes equal or smaller than the average quadratic error which is present in the data the iteration is stopped. Both those quantities are summed over the number of different energies at which the CT scans are acquired. The optimum EM solution, the EM solution selected with the stopping rule and the conventional DCM results are compared in table II.
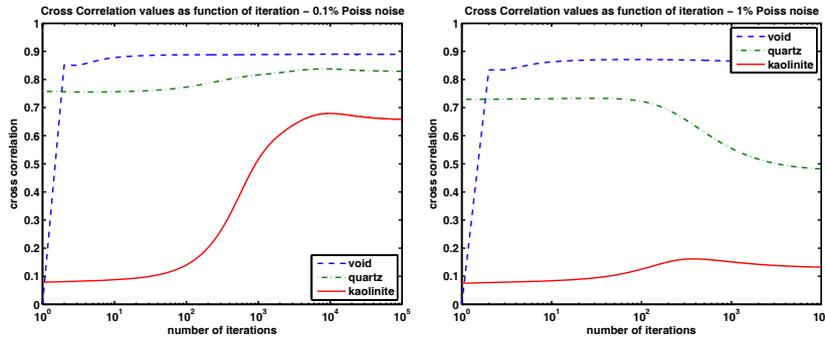

Fig. 2. – Cross-correlation, for each material, as a function of the number of iterations. The minimum and the maximum noise intensity are plotted.

TABLE II. – *Cross-correlation values (percent) for the various photon counting noises: EM optimum number of iterations (light gray), coventional DCM (medium gray), EM stopping rule (dark gray). In the case of 1% noise the stopping rule was not able to stop the iteration (the residual term did not reach the threshold in 10^5 iterations).*

	0.1%			0.4%			0.8%			1%		
void	89	89	89	88	87	88	88	83	87	87	81	—
quartz	84	83	82	77	66	73	74	55	63	74	50	—
kaolinite	68	66	56	33	28	33	19	17	19	13	13	—

The void is the best reconstructed material and a small number of iterations ($\sim 10^1$) is necessary to reach the maximum of the cross-correlation, even with 1% noise. The quartz and kaolinite components are fairly reconstructed with low noise (0.1%) while the accuracy for the kaolinite is poor with 1% noise. Note that after the optimum number of iterations (Cc^m is maximum) the solution starts to degenerate. This is due to the noise in the data, at a certain point during the iteration the algorithm starts to diverge from the best approximation. A comparison between the material distributions obtained with the method presented and with segmentation is finally shown in fig. 3. Note that the thresholding visualizes the void inclusion as encapsulated by kaolinite. This problem, even if not completely solved in the DCM plus EM approach, is less predominant.

5. – Conclusion

The expectation-maximization algorithm has been applied to the solution of the ill-posed linear system that has to be solved when a microstructure is to be determined following the data-constrained modeling approach. The attention has been focused on the material mixture that is typical for a hydrocarbon reservoir sandstone. The performance of the algorithm has been tested on a single, randomly generated voxel and on a numerical phantom. With the numerical sample, the whole process of CT data acquisition has
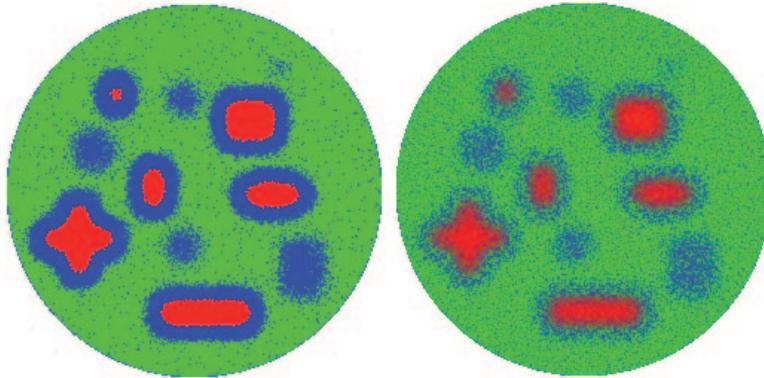

Fig. 3. – (Colour on-line) RGB representation of the computed volume fractions distributions (0.4% noise; R = void, G = quartz, B = kaolinite). On the left-hand side the CT scan at 30 keV has been thresholded using the mean values between the attenuation coefficient of the materials as the thresholds. On the right-hand side the result for the DCM plus EM is shown.

been simulated including photon counting statistical noise. When the noise is low the algorithm is capable to reconstruct both the matrix (quartz) and the inclusions (void and kaolinite) with good approximation. As the noise increases the accuracy for kaolinite is rapidly lost while for void and quartz it is still acceptable up to 1% noise. In the lower noise cases, the quality of the reconstructions is comparable with those obtained with conventional DCM. With respect to the thresholding, the reconstructed material distribution looks closer to the exact one in the voxels that effectively contain a mixture of materials.

REFERENCES

[1] DESRUES J., VIGGIANI G. and BÉSUELLE P., *Advances in X-ray Tomography for Geomaterials* (ISTE, London) 2006.
[2] ORTEGA J. A., ULM F.-J. and ABOUSLEIMAN Y., *Acta Geotech.*, **2** (2007) 155.
[3] MADADI MAHYAR, JONES ANTHONY C., ARNS CHRISTOPH H. and KNACKSTEDT MARK A., *Comput. Sci. Eng.*, **11** (2009) 65.
[4] YANG Y. S., TULLOH A., COLE I., FURMAN S. and HUGHES A., *J. Aust. Ceram. Soc.*, **43** (2007) 159.
[5] YANG Y. S., FURMAN S. and TULLOH A., *A data-constrained 3d model for material compositional microstructures*, in *Frontiers in Materials Science and Technology*, edited by BELL J., YAN C., YE L. and ZHANG L. (Trans. Tech. Publ.) 2008, pp. 267-270.
[6] YANG Y. S., GUREYEV T. E., TULLOH A., CLENNELL M. B. and PERVUKHINA M., *Meas. Sci. Technol.*, **21** (2010) 047001.
[7] VARDI Y. and LEE D., *J. R. Stat. Soc. B*, **55** (1993) 569.
[8] BERTERO MARIO and BOCCACCI PATRIZIA, *Introduction to Inverse Problems in Imaging* (Institute of Physics Publishing) 1998.
[9] `www.ts-imaging.net/services/appinfo/x-tract.aspx`.
[10] MOROZOV V. A., *Sov. Math. Dokl.*, **7** (1966) 414.